Journal of Zhejiang University SCIENCE A
ISSN 1009-3095 (Print); ISSN 1862-1775 (Online)
www.zju.edu.cn/jzus; www.springerlink.com
E-mail: jzus@zju.edu.cn

Investigation on Zener-Hollomon parameter in the warm-hot deformation behavior of 20CrMnTi*

YANG Hui†, LI Zhen-hong, ZHANG Zhi-liang

(*Department of Plasticity Technology, Shanghai Jiao Tong University, Shanghai 200030, China*)

†E-mail: aliceyangh@163.com

Received Nov. 24, 2005; revision accepted Mar. 6, 2006

Abstract: The warm-hot deformation behavior of 20CrMnTi steel was studied with hot compression tests at temperature range of 1123~1273 K and strain rate of 0.1~20 s^{-1}. The activation energy for warm-hot deformation is 426.064 KJ/mol. The influences of Zener-Hollomon parameter, strain and grain size imposing on the flow stress were analyzed in the temperature range of warm-hot forging. Creep theory and mathematical theory of statistics were used to obtain mathematical models of flow stress. The research and results provide scientific basis for controlling microstructure of forging process through Zener-Hollomon parameter.

Key words: Zener-Hollomon parameter, Warm-hot deformation, 20CrMnTi, Grain size
doi:10.1631/jzus.2006.A1453 **Document code:** A **CLC number:** TG312

INTRODUCTION

As one of the main forming materials for warm-forging accurate forming technology, 20CrMnTi cemented alloy steel is usually employed in the fabrication of wearable parts subjected to medium dynamic load, such as change gear, gear shaft, cross pin end, hub splines, etc., which are extensively adopted in the automobile industry. The application of warm forging technology (Hirschvogel and Dommelen, 1992; Sheljaskov, 1994; Shivpuri *et al*., 1994; Siegert *et al*., 1997; Lange, 1997) in industry has been increasingly expanded since its appearance in the 1970s. The temperature range of warm forging is 923~1123 K. Some kinds of steels cannot yield good deforming performance in warm forging because of poor metal flow causing various defects. Therefore, higher deformation temperature should be adopted for warm-hot deformation of these steel parts. Warm-hot deforming technology (Zhang, 1986) has particular advantage in precise deformation. Warm-hot deformation is carried out between hot deformation temperature and warm deformation temperature, which is 1123~1273 K for steel. Warm-hot deformation can employ controlling deforming technology different from traditional plasticity technology because of the higher temperature range used. Warm-hot controlling precise forging is a technology that can yield excellent external dimensional precision and good microstructure simultaneously through controlling deformation parameters in the deformation. In warm-hot controlling deforming technology, the quantitative relations of microstructure evolution and deformation parameters can provide theoretical foundation for numerical simulation and establishment of forming process and microstructure improvement. Zener-Hollomon parameter (Z) is an important physical quantity, with many studies indicating the great dependency of product quality and internal structure performance on Z (Hodgson, 1996).

At present, no systematic investigations on warm-hot forging process of 20CrMnTi steel have been reported (Poliak and Jonas, 2003; Venugopal *et al*., 2002; Elwazri *et al*., 2003; Cho *et al*., 2001; Serajzadeh *et al*., 2004), although a few studies have

* Project supported by the Shanghai Automotive Industry Science and Technology Development Fund, China

introduced microstructure parameter into creep theory equations via *Z* parameter. This study will investigate deforming behaviors of 20CrMnTi steel under warm-hot deformation temperature range and strain rate corresponding to practical production. This study is aimed at determining the activation energy for deformation, and the relations of *Z*, flow stress and dynamic recrystallization grain size, and developing mathematical models.

EXPERIMENTAL METHOD

The materials adopted for the tests are 20CrMnTi whose composition is given in Table 1.

Table 1 Chemical composition of 20CrMnTi steel

Component	wt%
C	0.17~0.23
Cr	1.00~1.30
Si	0.17~0.37
Cu	0.25
Mn	0.80~1.10
Ti	0.04~0.10
P	0.04
S	0.04

Thermo-mechanical experiments

The size of cylindrical compression specimens was Φ8 mm×12 mm. They were all in completely annealed state before being used in the experiments. The experimental equipment consisted of a Gleeble-3500 simulator. Argon was used to protect the specimens from surface oxidation. To minimize friction, thin graphite flakes were laid between punch head and billet head. Then, tests were carried out at different temperatures, strains and strain rates to determine how these variables influence the flow stress.

Continuous compression tests were conducted at strain rates ($\dot{\varepsilon}$) of 0.1, 0.5, 5, and 20 s^{-1} to a maximum true strain of 0.8, and at temperatures of 1123 K, 1173 K, 1223 K, and 1273 K on the Gleeble-3500 (shown schematically in Fig.1). The specimens were heated to 1273 K at a heating rate of 10 K/s, held for 5 min to eliminate thermal gradients, then cooled at 5 K/s to the deformation temperature, and deformed at the selected constant temperature.

The specimens were quenched after deformation.

Metallographic experiments

Sections were cut from the specimens along the longitudinal axis, and then the center areas of the specimens were used for metallographic analysis. The surfaces were prepared by mechanical polishing followed by etching in hot supersaturated picric acid, and then examined by optical microscopy.

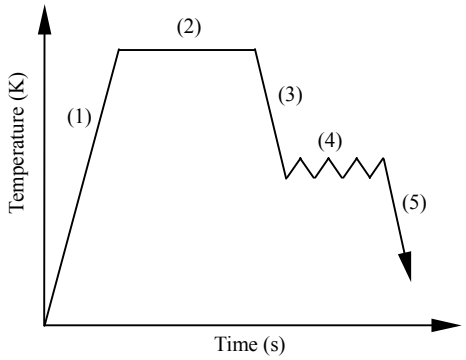

Fig.1 Schematic diagram of hot compression test
(1) Specimens reheated to 1283 K at a rate of 10 K/s; (2) Held for 5 min at 1283 K; (3) Cooled to the deformation temperature at a rate of 5 K/s; (4) Deformed at constant temperatures (1273 K, 1223 K, 1173 K, 1123 K); (5) Quenched rapidly after deformation

RESULTS AND DISCUSSION

Flow stress during warm-hot deformation

True stress/true strain curves of 20CrMnTi at different temperatures and strain rates are shown in Fig.2. The peak stress and peak strain of 20CrMnTi with varied influencing factors are shown in Table 2. In Soften Mechanism column of Table 2, A and B denote DRX and dynamic recovery, respectively.

Table 2 shows that: peak flow stress rapidly increases with increase of deformation rate. The average peak stress was 147.81, 169.37, 203.60 and 228.45 MPa when deformation rate $\dot{\varepsilon}$ was 0.1, 0.5, 5 and 20 s^{-1}, respectively. When $\dot{\varepsilon}$=20 s^{-1}, the average peak stress was 54.6% higher than that of $\dot{\varepsilon}$=0.1 s^{-1}. Peak flow stress increased with decreased deforming temperature. The average peak stress was 149.86, 169.04, 173.18 and 230.15 MPa when absolute temperature *T* was 1273, 1223, 1173 and 1123 K, respectively. The value of 1123 K was 53.6% higher than that of 1273 K.

Fig.2 shows that: flow stress change of 20CrMnTi steel during warm-hot deformation was

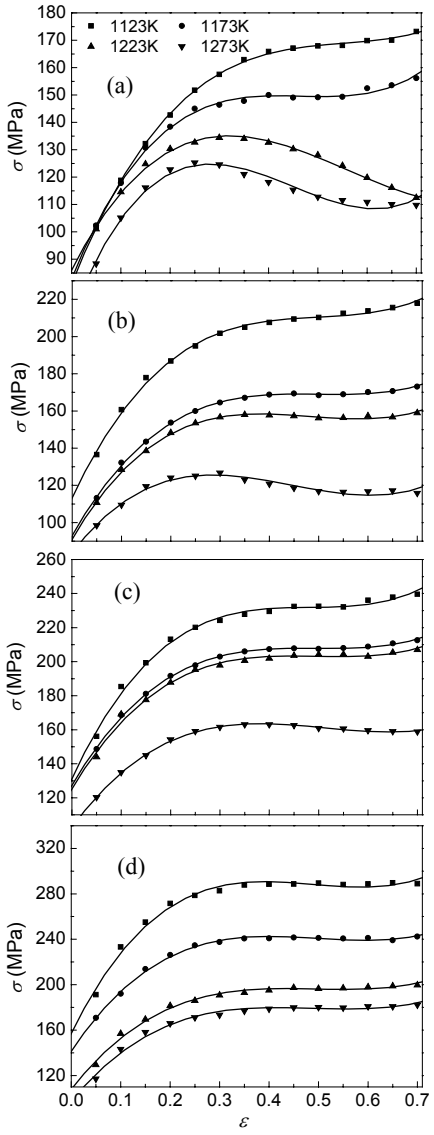

Fig.2 Effect of deformation temperature on the flow stress of 20CrMnTi steel deformed at strain rates of (a) 0.1 s^{-1}; (b) 0.5 s^{-1}; (c) 5 s^{-1}; (d) 20 s^{-1}

quite complicated. The σ-ε curve of 20CrMnTi steel could be divided into two forms, single-peak dynamic recrystallization and dynamic recovery. The higher temperature and lower strain rate facilitated recrystallization. With the increase of temperature and decrease of strain rate, flow stress of materials decreases. When T≤1173 K, the flow stress curve underwent dynamic recovery. With increase of ε during deformation, work hardening and dynamic softening occurred simultaneously. The work hardening dominant at the beginning of deformation, sharply increased the flow stress; hardening and softening reached balance

Table 2 Peak stress and peak strain of 20CrMnTi with varied influencing factors

$\dot{\varepsilon}$ (s^{-1})	T (K)	Soften mechanism	ε_p	σ_p (MPa)
0.1	1123	B	0.80	173.25
	1173	B	0.80	156.16
	1223	A	0.30	136.21
	1273	A	0.27	125.63
0.5	1123	B	0.80	218.01
	1173	B	0.80	173.11
	1223	A	0.34	158.83
	1273	A	0.28	127.52
5	1123	B	0.80	239.61
	1173	B	0.80	212.59
	1223	B	0.80	198.06
	1273	A	0.55	164.13
20	1123	B	0.80	289.73
	1173	B	0.80	242.31
	1223	B	0.80	199.60
	1273	B	0.80	182.16

when deformation reached a certain degree, flow stress value reached stable stress value. When T≥1223 K and $\dot{\varepsilon}$≤5, the flow stress curve indicated dynamic recrystallization. With the increase of ε during deformation, work hardening and dynamic recovery softening occurred simultaneously. The work hardening dominant at the beginning of deformation, sharply decreased flow stress; when deformation reached a certain degree, dynamic recrystallization softening will occur and decrease the flow stress value, then work hardening and recrystallization softening would reach a certain balance, and flow stress value will reach stable stress.

Variance analysis of experimental data showed that the statistical parameter F of equivalent strain rate, temperature and equivalent strain was 25.69, 286.83 and 403.03, respectively. These three factors are all significant influencing factors, with the order of influencing degree being equivalent strain rate>deformation temperature>equivalent strain. The strain rate and deformation temperature are the most sensitive and main factors for technical control. In practical production, equivalent strain rate mainly depends on manufacturing equipments, so that the selection of deformation temperature and distribution of multi-procedure deformation are of vital importance.

It can be seen that the strain corresponding to the

peak flow stress increases with the decrease of temperature and the increase of strain rate when DRX serves as the main soften mechanism. The peak flow stress decreases slowly after the strain reached its peak value. Decreasing temperature and increasing strain rate will delay the onset of DRX. Peak strain ranges from 0.28 to 0.34.

Activation energy for deformation and *Z*

Activation energy Q of deformation (J/mol) is an important physical parameter serving as indicator of deformation difficulty degree in plasticity deformation theory and is given by

$$Q = -R\left.\frac{\partial(\ln\dot{\varepsilon})}{\partial(1/T)}\right|_{\sigma}. \tag{1}$$

High temperature deformation mechanics of metal material is developed on the basis of metal high temperature creep behavior investigation. Like high temperature creep, warm-hot forging of metal and alloy also undergoes a heat activation process controlling the strain rate whose deformation mechanism is an extension of creep mechanism under different strain levels. Strain rate of warm-hot forging and creep usually differ by several orders of magnitude, so that hot forging can be regarded as an extension of creep under high strain rate and high stress (Jonas *et al*., 1969). They have very similar deformation mechanism and softening mechanism, Arrhenius Eq.(2) of heat activation can be used to describe both mechanisms above:

$$\dot{\varepsilon} = Af(\sigma)\exp\left(-\frac{Q}{RT}\right), \tag{2}$$

where $f(\sigma)$ is the stress function which can be expressed by the following three formulas:

$$f(\sigma) = \sigma^{n_1},$$
$$f(\sigma) = \exp(n_2\sigma),$$
$$f(\sigma) = \left[\sinh(\alpha\sigma)\right]^{n_3}.$$

Take the logarithm of each side of Eq.(2), so

$$\ln\dot{\varepsilon} = \ln A + \ln f(\sigma) - \frac{Q}{RT}. \tag{3}$$

Then substitute the three expressions of $f(\sigma)$ into Eq.(3):

$$\ln\dot{\varepsilon} = \ln A + n_1\ln\sigma - \frac{Q}{RT}, \tag{4}$$

$$\ln\dot{\varepsilon} = \ln A + n_2\sigma - \frac{Q}{RT}, \tag{5}$$

$$\ln\dot{\varepsilon} = \ln A + n_3\ln(\sinh(\alpha\sigma)) - \frac{Q}{RT}, \tag{6}$$

where σ denotes flow stress equal to maximum values of flow stress (peak stress σ_p), or to flow stress of steady state (steady-state stress σ_s); $\dot{\varepsilon}$ is strain rate; α, n_1, n_2, A are material constants; based on experience, α is 0.012; n_3 is the hyperbolic sine exponent.

The above flow stress σ is usually adopted as peak stress or steady-state stress. There is no difference between peak stress and steady-state stress for the above-mentioned flow stress because they are equal when dynamic recovery warm-hot deformation flow stress behaviors are studied; while in DRX process, peak stress is unequal to steady-state stress. Many research results indicated peak stress and steady-state stress have linear relation, and that both peak stress and steady-state stress can be described by Z parameter (Sakai, 1995). In this paper flow stress in the above equations is adopted as peak stress (σ_p).

Effect of the strain rate on the flow stress of 20CrMnTi steel is shown in Fig.3 indicating that the relationship of peak stress and strain can be described very well using Eq.(5) among the three expressions of $f(\sigma)$. Fig.4 is the graph of the relation between reciprocal of temperature and σ_p.

The deformation activation energy Q was calculated by the following Eq.(7):

$$Q = \left[\frac{\partial(\ln\dot{\varepsilon})}{\partial\sigma_p}\right]_T\left[\frac{\partial\sigma_p}{\partial(1/T)}\right]_{\dot{\varepsilon}}R. \tag{7}$$

Values of the first term of the right hand side of Eq.(7) were determined from the $\ln\dot{\varepsilon}\sim\sigma_p$ relation. The slope of the relation for steel 20CrMnTi in the temperature range of 1123~1273 K was changed in a very narrow range from 0.0499 to 0.0795, with average value being 0.0668.

The second term on the right hand side of Eq.(7)

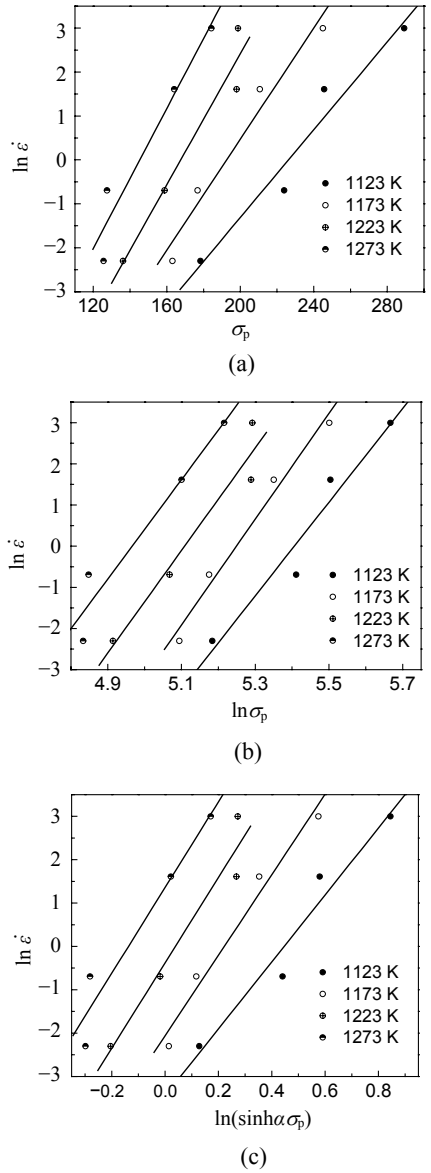

Fig.3 Effect of strain rate on the flow stress of 20CrMnTi steel in (a) $\ln\dot{\varepsilon}$ - σ_p; (b) $\ln\dot{\varepsilon}$ - $\ln\sigma_p$; (c) $\ln\dot{\varepsilon}$ - $\ln(\sinh\alpha\sigma_p)$

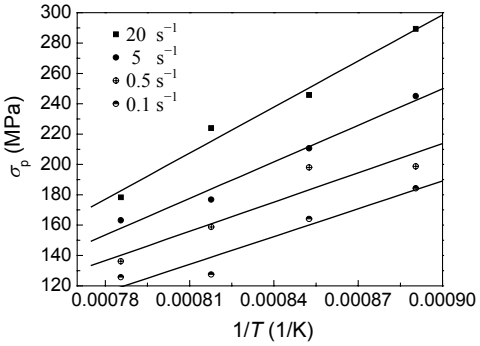

Fig.4 Effect of temperature on the flow stress of 20CrMnTi steel

was calculated from the σ_p~1/T relation. The slope of the relation for 20CrMnTi in the temperature range of 1123~1273 K was changed from 610801 to 1012000, with the average value being 767164.

The value of Q of 20CrMnTi at temperature 1123~1273 K is 426.064 kJ/mol. The apparent activation energy of 20CrMnTi steel is rather high. That is to say, when energy barrier is higher, the abilities of atom diffusion and grain boundary migration are weaker. As a result, dynamic recrystallization is easier to be excited.

Zener and Hollomon found that the stress-strain relation of steel depended on deformation temperature T and strain rate $\dot{\varepsilon}$, and that the relationship of T and $\dot{\varepsilon}$ can be denoted by a parameter Z:

$$Z = \dot{\varepsilon}\exp(Q/RT), \tag{8}$$

where T is deformation temperature (K); $\dot{\varepsilon}$ is strain rate (s^{-1}); R is the universal gas constant (R=8.314 J/(mol·K)); Z is Zener-Hollomon parameter, the physical meaning of which is the so-called temperature-compensated strain rate.

The values of ln$Z$ of 20CrMnTi steel under warm-hot temperature are listed in Table 3 showing that the values of ln$Z$ increase with decrease of temperature and increase of strain rate.

Table 3 Values of ln$Z$ of 20CrMnTi steel under different deformation conditions

$\dot{\varepsilon}$ (s^{-1})	T (K)			
	1273	1223	1173	1123
0.1	36.601	38.191	39.917	41.797
0.5	38.210	39.800	41.527	43.407
5	40.513	42.103	43.829	45.709
20	41.999	43.490	45.216	47.095

Flow stress and Z

The above-mentioned studies showed that

$$\dot{\varepsilon} = A\exp(n_2\sigma)\exp\left(-\frac{Q}{RT}\right). \tag{9}$$

Substitution of Eq.(9) into Eq.(8) yields

$$Z=A\exp(n_2\sigma).$$

Take the logarithm of each side, then

$$\sigma=(\ln Z-\ln A)/n_2=14.97\ln Z-464.35. \tag{10}$$

Therefore, the flow stress value under various deformation conditions can be calculated by Z parameter expression when such material constants as A, n_1, etc. are known. However, because Arrhenius equation is based on creep theory, Eq.(10) is only suitable for steady-state hot forging in practice. Its value can be used for loading calculation, equipment selection and so on. As to microstructure evolvement, especially recrystallization process, the above-mentioned flow stress model is obviously unsuitable. Therefore, we carried out the following investigation.

Zener and Sellars considered that during high temperature deformation process, flow stress of materials is related to deformation temperature, deformation rate and stress, and proposed a general expression material flow stress model:

$$\sigma = \sigma(\dot{\varepsilon}, T, \varepsilon),$$

where σ is flow stress; $\dot{\varepsilon}$ is equivalent strain rate; ε is equivalent strain; T is deformation temperature.

$$\left.\begin{aligned}\sigma &= f_1(\dot{\varepsilon}, T, \varepsilon)\\ Z &= f_2(\dot{\varepsilon}, T)\end{aligned}\right\} \Rightarrow \sigma = f(\ln Z, \varepsilon)$$
$$= [B_0 + B_1 \ln Z + B_2 (\ln Z)^2](A_0 + A_1\varepsilon + A_2\varepsilon^2 + A_3\varepsilon^3)$$
$$= F_1 F_2, \qquad (11)$$

among which

$$F_1 = B_0 + B_1 \ln Z + B_2 (\ln Z)^2,$$
$$F_2 = A_0 + A_1\varepsilon + A_2\varepsilon^2 + A_3\varepsilon^3,$$
$$A_i = g_i(\ln Z), \quad i = 0,\ 1,\ 2,\ 3.$$

Using Taylor expansion, any function can be written as a polynomial expression composed of power functions, so analysis and regression of experimental data can be used to obtain the warm-hot deformation flow stress model Eq.(11) of 20CrMnTi steel, with the value of each parameter as shown in Table 4.

Table 4 Polynomial regression result of flow stress (ln$Z$)

Parameter	Value
B_0	9.58
B_1	−0.41
B_2	0.0048
A_0	7.72ln$Z$−217.15
A_1	37.68ln$Z$−1069.23
A_2	−62.14ln$Z$+1526.57
A_3	38.87ln$Z$−896.13

The predicted values of flow stress are plotted against the measured flow stress values in Fig.5 showing that the prediction is reasonably good. But when strain rate is 5 and 20 s^{-1}, predicted values of flow stress are a bit higher than the measured values; when deformation temperature is lower, predicted values of flow stress are a bit lower than the measured values, when deformation temperature is higher, predicted values of flow stress are a bit higher than the measured values.

Critical strain, grain size and Z

Grain sizes obtained by experiment are shown in Table 5. D_0 is original grain size before deformation, and D_1 is grain size after deformation.

According to studies of Sellars, Yada, Saito, Hodgson, Anelli, critical strain of hot deformation of C-Mn steel is given by

$$\varepsilon_c = 0.8\varepsilon_p = CD_0^m Z^n, \qquad (12)$$

where the ranges of parameter C, m and n are 3.68×10^{-4}~9.12×10^{-4}, 0.24~0.50 and 0.15~0.19, respectively. By regression of experimental data, parameter C, m and n in critical strain model of 20CrMnTi in warm-hot deformation are 1.41×10^{-6}, 2.39 and 0.18, respectively. It can be seen that the values of m and C are different from those of C-Mn steel.

Dynamic soften of the specimen deforms more easier under warm-hot conditions with increasing

Table 5 Grain sizes of 20CrMnTi steel under different deformation conditions (μm)

$\dot{\varepsilon}$ (s^{-1})	T=1273 K		T=1223 K		T=1173 K		T=1123 K	
	D_0	D_1	D_0	D_1	D_0	D_1	D_0	D_1
0.1	19.89	13.06	16.78	12.58	16.61	10.03	16.45	9.66
0.5	19.89	12.78	16.78	9.64	16.61	8.73	16.45	7.56
5	19.89	9.53	16.78	8.76	16.61	7.28	16.45	6.53
20	19.89	8.45	16.78	7.34	16.61	6.89	16.45	6.32

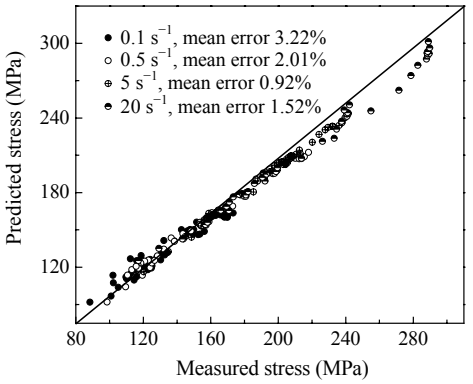

(a)

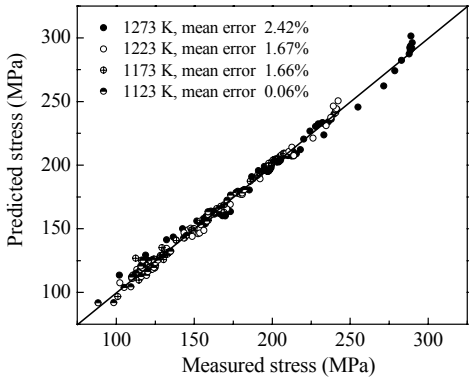

(b)

Fig.5 Comparison of predicted flow stress and measured flow stress at different strain rates (a) and different temperatures (b)

strain rate and deformation temperature decreases (i.e., with Z parameter value increasing). At the same time, dislocation density, deformation storage energy and recrystallization driving force increases, then recrystallization accelerates. As a result, recrystallization volume fraction is increased and austenite grain size is decreased. Experimental data showed that grain size of DRX is related to Zener-Hollomon parameter. The higher the parameter Z, the finer the austenitic grain size. With the increase of strain rate and decrease of deformation temperature, parameter Z will be increased and corresponding flow stress peak value will be higher. Under the same technical conditions, higher strain rate, original austenitic grain size will decrease austenitic grain size of DRX.

By the regression of experimental data, $\ln B$ and m_1 can be obtained as 5.267 and 0.098, respectively.

$$\ln D = \ln B - m_1 \ln Z . \quad (13)$$

Substitute Eq.(13) into built flow stress model Eq.(11) to obtain flow stress functions which can directly reflect microstructure evolution:

$$\sigma = f(\ln D, \varepsilon) = (E_1 \ln D + E_0)(F_0 + F_1\varepsilon + F_2\varepsilon^2 + F_3\varepsilon^3) . \quad (14)$$

By Eq.(14) with value of each parameter shown in Table 6, we can connect grain size after warm-hot deformation with deformation parameter, and realize microstructure control of warm-hot deformation by controlling Zener-Hollomon parameter. This paper has established the mechanical theory for further investigation.

Table 6 Polynomial regression results of flow stress (ln$D$)

Parameter	Value
E_0	1.0696
E_1	−0.0347
F_0	−107.04lnD+331.67
F_1	−378.26lnD+1314.28
F_2	578.16lnD−2371.93
F_3	−296.22lnD+1437.46

CONCLUSION

(1) Warm-hot deformation activation energy of 20CrMnTi steel is 426.064 KJ/mol.

(2) Taking Z as parameter, a mathematical model of steady flow stress given by Eq.(10) for warm-hot deformation of 20CrMnTi steel has been established and this model is incorporated in the following creep constitutive equation:

$$Z = A\exp(n_2\sigma_p).$$

(3) Grain size model of austenitic grain and critical strain model as given by Eq.(15) and Eq.(16) have been established with Z as parameter.

$$\varepsilon_c = 1.41\times10^{-6} D_0^{2.39} Z^{0.18} , \quad (15)$$

$$D = 193.83 Z^{-0.098} . \quad (16)$$

(4) A flow stress functions reflecting microstructure evolution given by Eq.(14) has been built based on parameter Z.

ACKNOWLEDGEMENT

The authors sincerely thank Engineer Huang Xuchuan for his valuable assistance in the hot deformation tests, and Dr. Xiao Hongsheng for his help with the optical microscopy.

References

Cho, S.H., Kang, K.B., Jonas, J.J., 2001. Mathematical modeling of the recrystallization kinetics of Nb microalloyed steels. *ISIJ International*, **41**(7):766-773.

Elwazri, A.M., Wanjara, P., Yue, S., 2003. Dynamic recrystallization of austenite in microalloyed high carbon steels. *Materials Science and Engineering A*, **339**(1-2):209-215. [doi:10.1016/S0921-5093(02)00164-8]

Hirschvogel, M., Dommelen, H., 1992. Some applications of cold and warm forging. *Journal of Materials Processing Technology*, **35**(3-4):343-356. [doi:10.1016/0924-0136(92)90326-N]

Hodgson, P.D., 1996. Microstructure modelling for property prediction and control. *Journal of Materials Processing Technology*, **60**(1-4):27-33. [doi:10.1016/0924-0136(96)02304-7]

Jonas, J. J., Sellars, C., Tegart, M., 1969. Strength and stucture under hot working conditions. *Int. Metallurgical Reviews*, **14**:1-24.

Lange, K., 1997. Modern metal forming technology for industrial production. *Journal of Materials Processing Technology*, **71**(1):2-13. [doi:10.1016/S0924-0136(97)00113-1]

Poliak, E.I., Jonas, J.J., 2003. Critical strain for dynamic recrystallization in variable strain rate hot deformation. *ISIJ International*, **43**(5):692-700.

Sakai, T., 1995. Dynamic recrystallization microstructures under hot working conditions. *Journal of Materials Processing Technology*, **53**(1-2):349-361. [doi:10.1016/0924-0136(95)01992-N]

Serajzadeh, S., Mirbagheri, S.M.H., Taheri, A.K., Zebarjad, S.M., 2004. Modelling of metal flow during hot forging with regard to microstructural aspects. *International Journal of Machine Tools and Manufacture*, **44**(14):1537-1545. [doi:10.1016/j.ijmachtools.2004.04.015]

Sheljaskov, S., 1994. Current level of development of warm forging technology. *Journal of Materials Processing Technology*, **46**(1-2):3-18. [doi:10.1016/0924-0136(94)90099-X]

Shivpuri, R., Babu, S., Kini, S., Pauskar, P., Deshpande, A., 1994. Recent advances in cold and warm forging process modeling techniques: selected examples. *Journal of Materials Processing Technology*, **46**(1-2):253-274. [doi:10.1016/0924-0136(94)90114-7]

Siegert, K., Kammerer, M., Keppler-Ott, T., Ringhand, D., 1997. Recent developments on high precision forging of aluminum and steel. *Journal of Materials Processing Technology*, **71**(1):91-99. [doi:10.1016/S0924-0136(97)00153-2]

Venugopal, S., Mannan, S.L., Rodriguez, P., 2002. Optimum design of a hot extrusion process for AISI type 304L stainless steel using a model for the evolution of microstructure. *Modelling and Simulation in Materials Science and Engineering*, **10**(3):253-265. [doi:10.1088/0965-0393/10/3/301]

Zhang, Z.L., 1986. Warm Forging Technology. Shanghai Science and Technology Publishing House, Shanghai, p.2-38 (in Chinese).